



PCCP

**Molecular mechanism of the triplet states formation in
bodipy-phenoxazine photosensitizer dyads confirmed by ab
initio prediction of the spin polarization**

Journal:	<i>Physical Chemistry Chemical Physics</i>
Manuscript ID	CP-ART-08-2024-003386.R1
Article Type:	Paper
Date Submitted by the Author:	17-Oct-2024
Complete List of Authors:	Kosaka, Maria; Kyoto University Graduate School of Science Faculty of Science Department of Chemistry Miyokawa, Katsuki; Kyoto University Kurashige, Yuki; Kyoto University, Graduate School of Science, Department of Chemistry

SCHOLARONE™
Manuscripts

Molecular mechanism of the triplet states formation in bodipy-phenoxazine photosensitizer dyads confirmed by *ab initio* prediction of the spin polarization

Maria Kosaka,^{*,†} Katsuki Miyokawa,[†] and Yuki Kurashige^{*,†,‡,¶}

[†]*Department of Chemistry, Graduate School of Science, Kyoto University, Kitashirakawa Oiwake-cho, Sakyo-ku Kyoto, 606-8502, Japan*

[‡]*FOREST, JST, Honcho 4-1-8, Kawaguchi, Saitama 332-0012, Japan*

[¶]*CREST, JST, Honcho 4-1-8, Kawaguchi, Saitama 332-0012, Japan*

E-mail: kosaka@theoc.kuchem.kyoto-u.ac.jp; kura@kuchem.kyoto-u.ac.jp

Abstract

Efficient formations of excited triplet states on the metal-free photosensitizer dyads, bodipy-phenoxazine (BDP-PXZ) and tetramethylbodipy-phenoxazine (TMBDP-PXZ), were investigated by *ab initio* calculations. We revealed the reason why two different triplet transient species, ^3CT and ^3BDP , can co-exist only for BDP-PXZ as observed in the previous study with the TR-EPR measurements. It was found that the state mixing of ^3CT enables the transition from ^1CT to ^3CT and ^3BDP states only for BDP-PXZ. This mixing effect is commonly seen in the singlet states of twisted intermolecular charge transfer molecules, though the key factor that determines the mixing of the excited states of the dyes was found to be the electron-donating ability of the substituents rather than their steric hindrance. The mechanism was corroborated by comparing

the spin polarization ratio of the triplet spin-sublevels measured by the TR-EPR with the theoretical predictions. The spin polarization ratio of the triplets should contain information about the transition *via* intersystem crossing, e.g. the twisted angle of two chromophores of the dyad, and thus it can be a powerful tool to analyze the molecular mechanism of photochemical processes at the electronic structure level. These insights on molecular structures' effect provided by this theoretical study would be a compass to molecular design for metal-free triplet photosensitizers.

1 Introduction

Triplet excited states of organic chromophores are one of the most familiar paramagnetic species in chemistry. Because their radiative and non-radiative decay to the ground state is spin-forbidden processes, it usually has a long enough lifetime to collide with or transfer the energy to other molecules, which allows for a wide range of applications, e.g., photon up-conversion,¹⁻⁵ triplet sensitizer,⁶⁻¹⁰ and dynamic nuclear polarization,¹¹⁻¹⁴ etc. Conversely, the generation of triplet excited states of metal-free organic chromophores by photo irradiation is not so efficient because the spin-orbit coupling (SOC) which induces the intersystem crossing (ISC) from S_1 state to T_n state is usually small, except for a few cases. One such exception is the transition between $n-\pi^*$ and $\pi-\pi^*$ excited states, in which the transition between in-plane and out-of-plane $2p$ orbitals on an atom generates angular momentum, but there is a limited variety of organic chromophores with low-lying $n-\pi^*$ excited states.

The spin-orbit coupling induced by charge transfer (SOCT)^{15,16} in covalently linked aromatic molecules is a promising alternative mechanism that can generate triplet states of a wide range of chromophores. For example, The unsubstituted boron-dipyrromethene (BDP) and its derivatives have attracted attention for their unique properties.^{17,18} They have high fluorescence quantum yields often approaching one, and thus it is difficult to obtain a sufficient quantity of triplets by photo irradiation. Filatov and co-workers have successfully obtained the triplet excited state of BDP in their pioneer work using the SOCT-ISC mech-

anism.¹⁹ A necessary condition for the SOCT should be that the energy levels of the singlet and triplet charge transfer states, i.e. ^1CT and ^3CT , lie between that of the singlet and triplet local excited states, ^1BDP and ^3BDP in this paper, and thus it should be valuable if we can predict energy levels of the excited states along the decay process by theoretical calculations.

To predict photochemical processes on covalently linked donor-accepter systems is still challenging because the characters of low-lying excited states drastically vary with the twist angle between the molecules, though it is hardly measurable with only a few exceptions²⁰ despite its importance. The locally excited (LE) state responsible for the absorption/emission of photons is stabilized in planar conformation whereas the charge transfer (CT) state, which is sensitive to the polarity of the environment, is stabilized in perpendicular conformation, and what complicates the situation is that these states can be mixed at the angle where they are close in energy. At the same time, it can be a strength if its character is well-designed. The sensitivity of luminescence properties of the twisted intramolecular charge transfer (TICT) state is used for sensing environmental polarity, microenvironmental viscosity, and chemical species.^{21,22} For highly efficient thermally activated delayed fluorescence materials (TADF) for organic light-emitting diodes (OLED), the CT character can make the S_1 - T_1 gap small, which enhances the reverse ISC, and the LE character will compensate for the lack of fluorescence efficiency.²³⁻²⁶ For SOCT-ISC molecules, the subject of this study, the twist angle should also alter the SOC between the singlet and triplet excited states; thus, a detailed theoretical analysis based on the molecular structure is necessary.

Here, molecular mechanisms of the triplet state formations in the bodipy-phenoxazine (BDP-PXZ) dyads were investigated by quantum chemical calculations. Interestingly, it has been suggested that a small modification, an addition of the methyl groups, of the BDP moiety prevents the generation of ^3CT state, while it was generated together with ^3BDP state when the substituents were absent.²⁷ It was also suggested that ^3CT and ^3BDP states exhibit different EPR patterns, i.e., different spin polarizations, which should contain the information

of the spin-selective ISC where the molecules went through,²⁸ e.g. the twisted angle between the chromophores, and can be used for the corroboration of the proposed mechanism by comparing with the theoretical predictions. However, it has not been established to predict the spin polarization in the magnetic axis for the triplet states of organic chromophores because the quantitative calculations of the zero-field splitting (ZFS) D-tensor are necessary. Our recent development for the prediction of the spin-spin coupling (SSC)²⁹ based on the *ab initio* density-matrix renormalization group (DMRG) algorithm opened up the possibility of quantitative prediction for the magnetic properties of organic chromophores. By comparing the theoretical prediction with the TR-EPR experiments, therefore, we can confirm the character of the transient species and the mechanism at the electronic structure level.

2 Computational Details

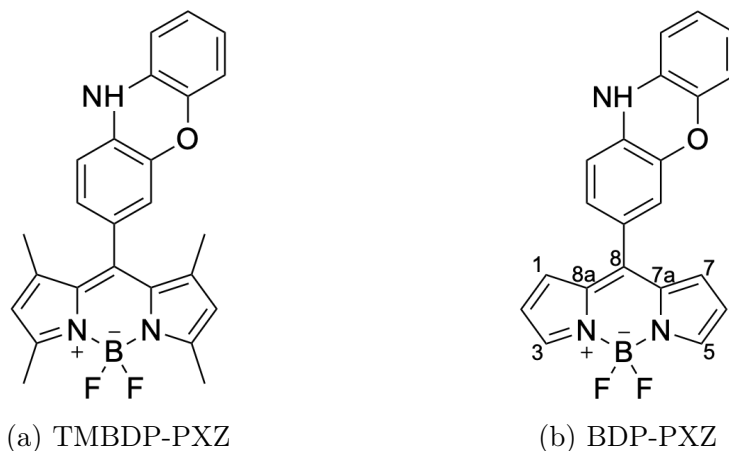


Figure 1: Chemical structures of BDP-PXZ , TMBDP-PXZ

Bodipy-phenoxazine dyads shown in Figure 1, which are modeled by replacing the C_4H_9 alkyl-chain with a hydrogen atom for the dyads synthesized in the experiment,²⁷ were adopted in this study. Geometry optimizations were performed with the def2-TZVP basis sets³⁰⁻³² and a long-range corrected BLYP functional³³ (LC-BLYP) in which the range separation parameter was tuned to $\mu = 0.15$ was adopted (see SI). The polarizable continuum model³⁴ (PCM) was used to account for the solvent effect of toluene. All the excited states

including the lowest triplet state were calculated by the time-dependent density functional theory (TD-DFT) using the ORCA5 program package.³⁵

The matrix elements of spin-orbit coupling between the ¹CT and each spin sublevel (x, y, z axes of the molecular frame) of ³CT and ³BDP states were calculated by TD-DFT. The ZFS D-tensor was calculated by the method developed in Ref[29], in which the expectation values of the spin-spin coupling operator in the Breit-Pauli Hamiltonian

$$\hat{H}_{\text{SSC}} = \frac{g_e^2 \mu_B^2 \alpha^2}{2} \sum_{i \neq j} \left[\frac{\hat{\mathbf{s}}(i) \cdot \hat{\mathbf{s}}(j)}{r_{ij}^3} - \frac{3(\hat{\mathbf{s}}(i) \cdot \mathbf{r}_{ij})(\hat{\mathbf{s}}(j) \cdot \mathbf{r}_{ij})}{r_{ij}^5} \right], \quad (1)$$

where g_e is electron g-factor, μ_B is Bohr magneton, α is fine structure constant, $\hat{\mathbf{s}}(i)$ is the spin operator of an electron i and \mathbf{r}_{ij} is the distance between electrons i and j , were calculated by the contraction of the spin-spin coupling integrals d_{pqrs}^{kl} and the spin-dependent two-particle density matrices q_{pqrs} (2-RDM) as

$$D_{kl}^{\text{SSC}} = \frac{g_e^2 \alpha^2}{4S(2S-1)} \sum_{pqrs} d_{pqrs}^{kl} q_{pqrs}, \quad (2)$$

where

$$d_{pqrs}^{kl} = \iint \phi_p(\mathbf{r}_1) \phi_r(\mathbf{r}_2) \frac{r_{12}^2 \delta_{kl} - 3(\mathbf{r}_{12})_k (\mathbf{r}_{12})_l}{r_{12}^5} \phi_q(\mathbf{r}_1) \phi_s(\mathbf{r}_2) d\mathbf{r}_1 d\mathbf{r}_2, \quad (3)$$

$$q_{pqrs} = \frac{1}{4} \langle \Psi | E_{pq} \delta_{sr} - S_{ps}^z S_{rq}^z + \frac{1}{2} (S_{pq}^z S_{rs}^z - E_{pq} E_{rs}) | \Psi \rangle. \quad (4)$$

The density matrix renormalization group self-consistent field (DMRG-SCF) theory³⁶⁻³⁸ was used as a reference wavefunction of the spin-dependent 2-RDM were calculated. The spin-spin coupling integrals were efficiently calculated with the resolution of the identity (RI) approximation³⁹ implemented in the modified version of the PySCF library.⁴⁰ Once D-tensor was calculated, the 3×3 tensor was diagonalized to obtain the energy gaps of the spin-sublevels that correspond to the D and E values with the sing convention of ESR experiment.

3 Results

3.1 Molecular mechanism of the formation of the triplet states

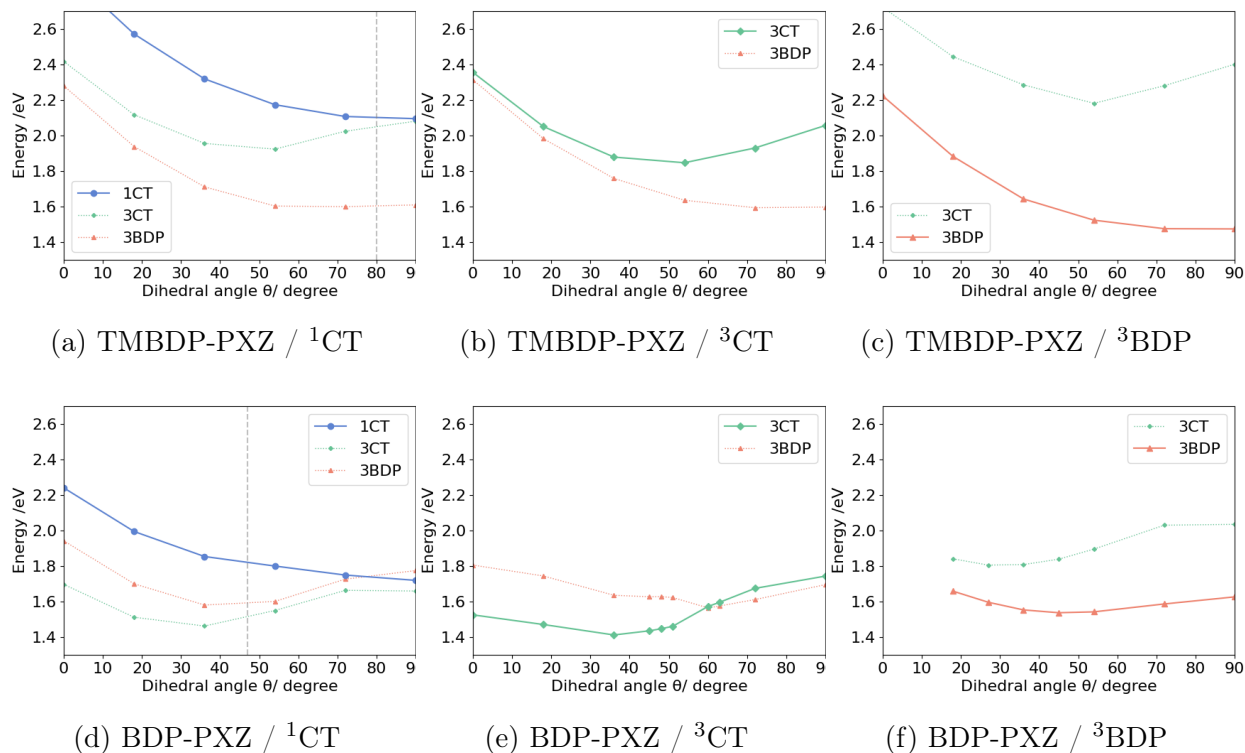


Figure 2: Potential energy curves of ^1CT , ^3CT , and ^3BDP states along the dihedral angle between BDP and PXZ moieties, calculated with LC-BLYP/def2-TZVP under solvent effect of toluene by LR-CPCM. The geometries were optimized for ^1CT :(a),(d), ^3CT :(b),(e), ^3BDP :(c),(f) states of BDP-PXZ and TMBDP-PXZ with constraints for the dihedral angle θ between BDP and PXZ moieties. The target state is depicted with solid lines, while others with dotted lines; the former was calculated with equilibrium solvent and the latter with non-equilibrium solvent. The gray dashed lines in (a) and (d) indicate the θ for the ground state stabilized structure.

To elucidate the molecular mechanism of the formation of the triplet states, we performed the geometry optimization for ^1CT , ^3CT , and ^3BDP states with constraints for the dihedral angle θ between BDP and PXZ moieties. Figure 2 shows the potential energy curves (PECs) of TMBDP-PXZ and BDP-PXZ in toluene along the dihedral angle θ . The dihedral angle of TMBDP-PXZ at the equilibrium structure of the ground state was found to be $\theta =$

80°, i.e., BDP and PXZ are almost perpendicular due to the steric hindrance of the CH₃ groups, while that of BDP-PXZ was $\theta = 47^\circ$. In both systems, after the photo irradiation θ will increase along the slope of the ¹CT state towards $\theta = 90^\circ$, where the ¹CT and ³CT states are energetically very close due to the small exchange coupling for the perpendicular conformation. The shapes of PECs of ¹CT and ³CT are similar for TMBDP-PXZ and BDP-PXZ systems, but that of ³BDP state is significantly different by the presence and absence of the CH₃ group; the perpendicular structure ($\theta \simeq 90^\circ$) is energy minimum in TMBDP-PXZ but is unstable in BDP-PXZ. In fact, at the perpendicular structure, the energy level of ³BDP is lower by 0.4 eV than ¹CT and ³CT states for TMBDP-PXZ, in contrast, though it is very close in energy to ¹CT and ³CT states for BDP-PXZ and as will be discussed ³BDP and ³CT are strongly mixed at around $\theta = 90^\circ$.

In TMBDP-PXZ system, after the transition to either ³BDP or ³CT state the wavepackets will immediately decay to the ³BDP state, which lies at lower energy than ³CT state even in the solvent environment that minimizes the energy level of ³CT as shown in Fig 2b. In BDP-PXZ system, the wavepackets that transit to the ³CT state can stay on the ³CT potential energy surface because ³CT has lower energy than ³BDP in the solvent reorganized for the ³CT state, and the wavepacket that directly transit to the ³BDP state from ¹CT state will stay in the ³BDP state because it is lower in energy than ³CT in the solvent reorganized for the ³BDP state. This should be the reason why only the BDP-PXZ system exhibits the dual components TR-EPR spectra while TMBDP-PXZ does not. Note that the state-specific effects, which can be evaluated by the corrected LR method^{41,42} for example, were neglected in the calculations based on the LR-CPCM method. It may stabilize the excited states with the CT character and make it easier for ³CT and ³BDP to coexist. The detailed analysis for the difference in energetics caused by the CH₃ groups will be discussed in Sec.3.4

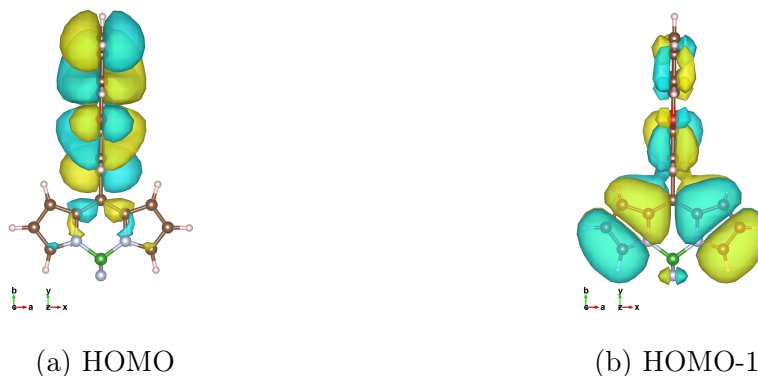


Figure 3: Surface plots of canonical MOs (isovalue=0.008), calculated with LC-BLYP/def2-TZVP under solvent effect of toluene by LR-CPCM, non-equilibrium condition.

Table 1: The SOC matrix elements $\langle {}^1\text{CT} | H_{\text{soc}} | {}^3\text{CT}_\mu \rangle$ and $\langle {}^1\text{CT} | H_{\text{soc}} | {}^3\text{BDP}_\mu \rangle$ for the TMBDP-PXZ and the BDP-PXZ, along with ΔE indicating the energy gaps (${}^1\text{CT} - {}^3\text{CT}$) and (${}^1\text{CT} - {}^3\text{BDP}$), calculated with LC-BLYP/def2-TZVP under solvent effect of toluene by LR-CPCM, non-equilibrium condition.

(a) TMBDP-PXZ							(b) BDP-PXZ						
θ	0°	18°	36°	54°	72°	90°	θ	0°	18°	36°	54°	72°	90°
$ \langle {}^1\text{CT} H_{\text{soc}} {}^3\text{CT}_\mu \rangle / \text{cm}^{-1}$							$ \langle {}^1\text{CT} H_{\text{soc}} {}^3\text{CT}_\mu \rangle / \text{cm}^{-1}$						
x	0.11	0.09	0.05	0.01	0.01	0.01	x	0.00	0.03	0.03	0.11	0.44	0.48
y	0.03	0.07	0.11	0.14	0.14	0.02	y	0.07	0.13	0.15	0.15	0.06	0.00
z	0.00	0.01	0.00	0.01	0.02	0.01	z	0.01	0.01	0.00	0.02	0.01	0.00
$\Delta E / \text{eV}$							$\Delta E / \text{eV}$						
	0.52	0.45	0.36	0.25	0.08	0.01		0.54	0.48	0.39	0.25	0.09	0.06
$ \langle {}^1\text{CT} H_{\text{soc}} {}^3\text{BDP}_\mu \rangle / \text{cm}^{-1}$							$ \langle {}^1\text{CT} H_{\text{soc}} {}^3\text{BDP}_\mu \rangle / \text{cm}^{-1}$						
x	0.29	0.39	0.47	0.56	0.66	0.71	x	0.22	0.33	0.40	0.52	0.52	0.56
y	0.13	0.11	0.08	0.03	0.03	0.01	y	0.04	0.02	0.01	0.03	0.05	0.00
z	0.02	0.01	0.03	0.03	0.04	0.01	z	0.02	0.02	0.00	0.03	0.01	0.00
$\Delta E / \text{eV}$							$\Delta E / \text{eV}$						
	0.66	0.63	0.61	0.57	0.51	0.49		0.30	0.29	0.27	0.20	0.02	-0.06

3.2 Spin polarization induced by intersystem crossing

To reveal the spin polarization axis in the molecular frame, which cannot be determined by the TR-EPR experiment for randomly oriented molecules, we computed the SOC matrix elements between ^1CT and ^3CT ($\langle ^1\text{CT} | H_{\text{soc}} | ^3\text{CT}_\mu \rangle$) and ^1CT and ^3BDP ($\langle ^1\text{CT} | H_{\text{soc}} | ^3\text{BDP}_\mu \rangle$) where $\mu = x, y, z$ at the structures on the PECs of ^1CT in Fig. 2a,2d. Table 1a and 1b show the SOC matrix elements of BDP-PXZ and TMBDP-PXZ, respectively, for each component $^3\text{CT}_x$, $^3\text{CT}_y$, and $^3\text{CT}_z$ where x , y , and z correspond to the molecular axis of BDP moiety shown in Fig. 3; the long axis is x , the short axis is y , and the out-of-plane axis is z . As shown in Table 1a, the SOC of $\langle ^1\text{CT} | H_{\text{soc}} | ^3\text{BDP}_\mu \rangle$ is x -polarized and significantly larger than that of $\langle ^1\text{CT} | H_{\text{soc}} | ^3\text{CT}_\mu \rangle$ at any dihedral angle θ .

Theoretically, the SOC is usually accounted by the change in the occupation of the atomic orbitals that have different angular momentum, e.g., the change in the occupation of $2p_y$ and $2p_z$ orbitals, such as a lone pair orbital and π orbital, of an atom will contribute x -polarized SOC. As far as we know, it has never been explicitly analyzed, but the SOC in linked π -conjugated systems should originate from the transition between the in-plane (σ orbital) and out-of-plane (π orbital) associated with a charge transfer excitation. For example, Fig. 3 shows the canonical molecular orbitals that represent most of the transition between ^1CT and ^3BDP at $\theta = 90^\circ$ structure. The transition appears to involve the difference in occupations of the $2p_x$ in HOMO and $2p_z$ in HOMO-1 of the C7a and C8a atoms. It causes the change in the angular momentum about the x -axis and is considered to be the origin of the x -polarized SOC of ^3BDP shown in Table 1a and 1b. This is an explanation for the mechanism of SOCT-ISC at the electronic level, i.e., the reason why the SOC matrix elements between the charge transfer state and locally excited state in linked π -conjugated molecules are significant. The mechanism should be universal for other covalently linked π -conjugated systems, e.g., the efficient reverse ISC of TADF. Note that the contribution from an atom that is directly linked to the other aromatic moiety, the C8 atom in this case, usually has the largest contribution to this type of the generation of SOC because the in-plane $2p_x$ or $2p_y$

of the linked atom, which has the same symmetry with the π orbitals of the other aromatic moiety, can strongly mix with those, but the C8 atom happens to be located at the node of π orbital of BDP in HOMO-1 and cannot contribute at least at the C_s ($\theta = 90^\circ$) structure.

For the same reasons, it is reasonable that the SOC matrix element $\langle {}^1\text{CT} | H_{\text{soc}} | {}^3\text{CT}_\mu \rangle$ for the TMBDP-PXZ is weak because the transition between ${}^1\text{CT}$ and ${}^3\text{CT}$ does not involve the change in electron configuration. It suggests that the direct transition from ${}^1\text{CT}$ to ${}^3\text{BDP}$, which exhibits larger couplings than those with ${}^3\text{CT}$ by one or two order magnitudes, can occur through the minimum energy crossing point (MECP), which should be displaced along other degree-of-freedom that is orthogonal to the minimum energy path of ${}^1\text{CT}$ shown in Figure 2a. In fact, we found that the MECP is located at $\theta = 87^\circ$ with less than 7 kcal/mol above the energy minimum of ${}^1\text{CT}$ state (see SI), so the direct transition to ${}^3\text{BDP}$ should be quite feasible. Note that the energy gap between ${}^3\text{BDP}$ and ${}^3\text{CT}$ should be small at around the MECP, and two triplet states can be strongly mixed and an ISC transition to ${}^3\text{CT}$ could be possible by borrowing the x -polarized SOC of ${}^3\text{BDP}$, although it should soon decay to the lower energy state ${}^3\text{BDP}$ anyway without changing the polarization in the molecular frame conserving the angular momentum. For BDP-PXZ, in which the mixture of two components observed in the TR-EPR spectra,²⁷ not only ${}^3\text{BDP}$ but also ${}^3\text{CT}$ should be generated although the transition from ${}^1\text{CT}$ to ${}^3\text{CT}$ is considered to be inefficient due to the weak coupling character as explained above. As can be seen in Table 1b, however, the SOC matrix element between ${}^1\text{CT}$ and ${}^3\text{CT}$ is large enough ($\sim 0.5 \text{ cm}^{-1}$) at around $\theta = 90^\circ$ structure. This should be explained by the state mixing of ${}^3\text{CT}$ and ${}^3\text{BDP}$; those are very close in energy at around $\theta = 90^\circ$ structure (Table 2d). Indeed, it was found that the electron configurations of ${}^3\text{CT}$ state obtained by TDDFT consist of 57.6 % HOMO of PXZ \rightarrow LUMO of BDP (${}^3\text{CT}$ configuration) and 38.7 % HOMO of BDP \rightarrow LUMO of BDP (${}^3\text{BDP}$ configuration). The latter configuration should contribute to the large x -polarized SOC of ${}^3\text{CT}$ in BDP-PXZ.

3.3 Prediction of the ZFS D-tensor in molecular frame

Table 2: ZFS of the triplet sublevels of ^3BDP and ^3CT , and the correspondence between the molecular axis x, y, z (Fig. 3) and magnetic axis x', y', z' for ^3BDP and x'', y'', z'' for ^3CT . The values are calculated with (28e, 25o) DMRG-CASSCF.

	D/mT	E/mT	Polarization
Calc			
^3BDP	-79.44	6.87	$x (= z')$
^3CT	-44.24	17.75	$x (= y'')$
Expt ^a			
^3BDP	-82.1	19.1	z'
^3CT	-37.5	8.2	y''

^a Ref[27].

The ZFS D-tensor in the molecular frame was calculated at the level of DMRG-CASSCF theory, in which the active space consists of the full valence π orbitals CAS(28e, 25o), and diagonalized to assign the magnetic axis in the molecular frame; the detail of the method is described in Ref[29]. Table 2 summarizes ZFS of the spin sublevels of ^3BDP and ^3CT for BDP-PXZ, and polarization axis with the correspondence between the molecular axis x, y, z and magnetic axis x', y', z' for ^3BDP and x'', y'', z'' for ^3CT . The ZFS parameters D and E values were predicted to be -79.44 mT and 6.87 mT for ^3BDP at the ^3BDP energy minimum structure and -44.24 mT and 17.75 mT for ^3CT at the ^3CT energy minimum structure, respectively. The predicted D values are in good agreement with the values determined by the TR-EPR spectra in Ref[27]. There are discrepancies in the trend between theoretical and experimental values for the E value, of which the absolute value is often small and sensitive to the change in the D-tensor.²⁹ In addition, the magnetic axis in the molecular frame was determined by diagonalizing the D tensor, and it was found that the x -axis, which is the axis of the electron polarization inducted by the spin-selective ISC from ^1CT (see Section 3.2), corresponds to the z' and y'' for ^3BDP and ^3CT , respectively. It is also consistent with the TR-EPR experiments, which strongly support the proposed molecular mechanism in Sec. 3.1

3.4 Insights into the molecular mechanism

As proposed by the theoretical calculations and confirmed by the consistency between the calculations and the experiments of the TR-EPR measurement, the transitions from ^1CT to ^3CT and ^3BDP should occur at around $\theta = 90^\circ$ structure, hence the steric hindrance by CH_3 groups of TMBDP-PXZ is not critical to the mechanism, rather the electron donor character of the groups, which should affect the energy levels of HOMO and LUMO of the BDP moiety, seems to be more important for the mechanism.

Regarding this point, the TD-DFT calculation for the BDP monomer was performed. As summarized in Table 3, when CH_3 groups were added, the both HOMO and LUMO energy of the BDP monomer increase by 0.67 eV and 0.45 eV, respectively, and the excitation energy of ^3BDP slightly decrease by 0.15 eV. It should have more impact on ^3CT because only the LUMO of BDP, which accepts the electron from the HOMO of the donor PXZ that should not be altered by the substitution of CH_3 to BDP moiety, is involved in the charge transfer.

Thus only the ^3BDP is observed for TMBDP-PXZ, whereas the ^3CT is observed together with ^3BDP for BDP-PXZ in the TR-EPR measurements.

Table 3: HOMO, LUMO, and T_1 excitation energies in eV of the BDP monomer, calculated with LC-BLYP/def2-TZVP under solvent effect of toluene by LR-CPCM, non-equilibrium condition.

	HOMO	LUMO	T_1
BDP	-7.44	-2.00	1.71
TMBDP	-6.76	-1.54	1.56

To ensure the impact of the electron-withdrawing/donating groups on BDP moiety, the potential energy curves were calculated for three other BDP-PXZ derivatives with different substituent groups X ($\text{X} = \text{Me}, \text{NO}_2, \text{and NH}_2$) on C3 and C5 atoms in BDP, where the groups bring insignificant steric effect to PXZ moiety. The curves have similar shapes throughout the θ , dihedral angle between BDP and PXZ moieties as reaction coordinates; however quite different in energy levels of ^3CT and ^3BDP (see SI).

Moreover, with a series of various substituent groups ($\text{X} = \text{F}, \text{Cl}, \text{NH}_2, \text{OMe}, \text{Me}, \text{H}$,

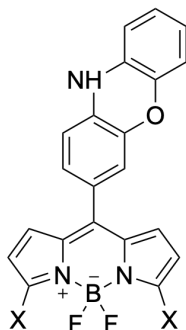


Figure 4: Chemical structures of BDP-PXZ derivatives with substituent groups X, as X = Me, NO₂, and NH₂ in potential energy curve analysis, and X = F, Cl, NH₂, OMe, Me, H, CF₃, Ac, CHO, CN, and NO₂ in Hammett substituent constant analysis.

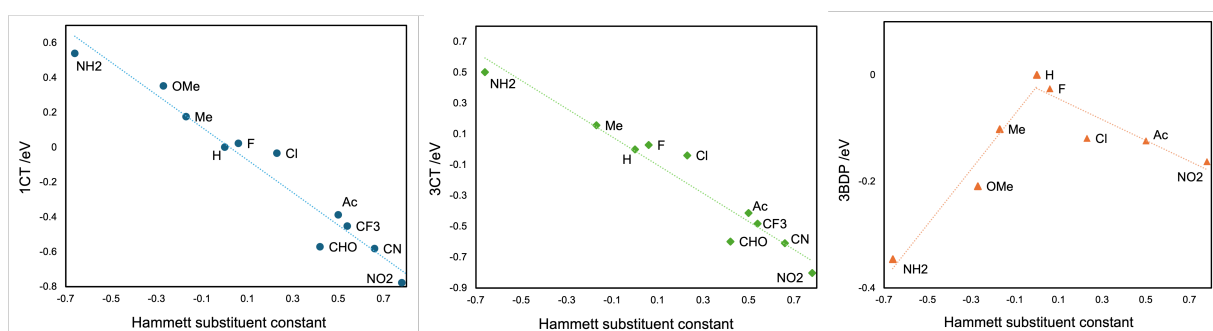


Figure 5: The scatter plot between Hammett substituent constants and the energy levels of ¹CT, ³CT, and ³BDP states for BDP-PXZ derivatives with a series of different substituent groups, calculated with LC-BLYP/def2-TZVP under the solvent effect of toluene by LR-CPCM, equilibrium condition.

CF₃, Ac, CHO, CN, and NO₂) on the C3 and C5 atoms of BDP moiety, the scatter plots between Hammett substituent constants and the energy levels of ¹CT, ³CT, and ³BDP states were obtained, as the positive substituent constants correspond to electron-withdrawing groups while the negatives to electron-donating.⁴³ The energy levels are calculated using the optimized structures under the constraints for the dihedral angle $\theta = 90^\circ$ for clarity. As shown in Figure 5, there were certain correlations between the substituent constant and ¹CT and ³CT energy levels; the correlation coefficient was -0.973 for ¹CT, and -0.967 for ³CT, respectively. This result makes it clear that the electron-donating groups on the C3 and C5 atoms of BDP raise the energy level of ^{1,3}CT states, as the BDP-LUMO level gets higher, and vice versa. On the other hand, the ³BDP level is the highest when X = H, and it gets lower for both electron-donating and withdrawing groups. It is natural, considering

that ^3BDP state involves not only BDP-LUMO but also BDP-HOMO. In this way, it was reasonably elucidated that the electron donor character of the groups, which should affect the energy levels of HOMO and LUMO of the BDP moiety, is more important for the formation mechanism of ^3CT and ^3BDP transient species, rather than their steric hindrance. The different dependencies of the CT and LE excited states on the substituent effects should be useful for designing molecules that meet the necessary condition of an efficient SOCT that the energy levels of the singlet and triplet charge transfer states lie between that of the singlet and triplet local excited states.

4 Summary

We revealed the detail of the triplet formation process of BDP-PXZ and TMBDP-PXZ *via* the SOCT-ISC; the reason why the two different triplet transient species were experimentally observed for the BDP-PXZ, and only one species for the TMBDP-PXZ, even though the structures differ only by the substitution of the methyl groups. As shown in the analysis of the potential energy curves along the dihedral angle between BDP and PXZ moieties as the reaction coordinates, in both molecules the transition from ^1CT to either ^3BDP or ^3CT state occurs at about the orthogonal conformation, where the ^1CT and ^3CT states are close in energy.

In BDP-PXZ, it was found that the wavepacket that transits to the ^3CT and ^3BDP states can remain on their adiabatic potential energy surface because both states are the lowest triplet states in their solvent environment. In TMBDP-PXZ, on the other hand, the ^3BDP state is more stable than ^3CT state even in the solvent environment that is optimized for ^3CT state, and only ^3BDP state will be observed regardless of which triplet excited state surfaces the wavepacket has at first transited to. The key to this difference is therefore not the steric hindrance, but the electric donating effect of the CH_3 groups on BDP moiety, which increases the energy levels of BDP's HOMO and LUMO to elevate the ^3CT .

Utilizing the correlation analysis between the energy levels of the excited states and Hammett substituent constants, it was reasonably elucidated that the electron-donating/withdrawing substituent groups on the BDP moiety are strongly correlated with $^1,^3\text{CT}$ states; and with ^3BDP , have an analogous trend with CT state for electron-withdrawing groups, while the opposite trend for electron-donating ones. It should be universal for the ^3CT and ^3BDP states of dyad systems and can be exploited to control the formation process of the triplet state by the SOCT-ISC.

Furthermore, with the calculation of the spin-orbit coupling matrix element between ^1CT and each triplet state, it was shown that the triplet states generated by the SOCT-ISC should be spin polarized to the component of the BDP's long axis ($^3\text{CT}_x$ and $^3\text{LE}_x$). This result, together with the prediction of the ZFS tensor in the molecular frame, is quite consistent with the TR-EPR spectra, which strongly supports the SOCT-ISC mechanism we propose. Our theoretical study has reasonably discovered the fundamental mechanisms of the triplet formation of BDP-PXZ systems and the effect of the molecular structures. These insights would be a compass to molecular design for metal-free triplet photosensitizers.

Author contributions

Y. K. conceived the project. M. K. carried out the calculations and analyzed computational results, and K. M. and Y. K. partly contributed to the calculations. M. K. and Y. K. participated in the composition and revision of the manuscript.

Conflicts of interest

There are no conflicts to declare.

Data availability

The data supporting this study's findings are available from the corresponding authors upon reasonable request.

Acknowledgement

This work was partly supported by the JST-FOREST Program (JPMJFR221R), JST-CREST Program (JPMJCR23I6), MEXT Q-LEAP Program (JPMXS0120319794), JSPS KAKENHI (JP23K26614), and Tokyo Ohka Foundation for The Promotion of Science and Technology. The computation was partly performed using the Research Center for Computational Science, Okazaki, Japan (Project: 24-IMS-C028).

References

- (1) Pérez-Ruiz, R. Photon Upconversion Systems Based on Triplet–Triplet Annihilation as Photosensitizers for Chemical Transformations. *Top Curr Chem (Z)* **2022**, *380*, 23.
- (2) Yanai, N.; Kimizuka, N. New Triplet Sensitization Routes for Photon Upconversion: Thermally Activated Delayed Fluorescence Molecules, Inorganic Nanocrystals, and Singlet-to-Triplet Absorption. *Acc. Chem. Res.* **2017**, *50*, 2487–2495.
- (3) Singh-Rachford, T. N.; Castellano, F. N. Photon Upconversion Based on Sensitized Triplet–Triplet Annihilation. *Coord. Chem. Rev.* **2010**, *254*, 2560–2573.
- (4) Zhou, J.; Liu, Q.; Feng, W.; Sun, Y.; Li, F. Upconversion Luminescent Materials: Advances and Applications. *Chem. Rev.* **2015**, *115*, 395–465.
- (5) Zhong, M.; Sun, Y. Recent Advancements in the Molecular Design of Deep-Red to near-Infrared Light-Absorbing Photocatalysts. *Chem Catalysis* **2024**, 100973.

- (6) Nguyen, V.-N.; Yan, Y.; Zhao, J.; Yoon, J. Heavy-Atom-Free Photosensitizers: From Molecular Design to Applications in the Photodynamic Therapy of Cancer. *Acc. Chem. Res.* **2021**, *54*, 207–220.
- (7) Zhang, X.; Wang, Z.; Hou, Y.; Yan, Y.; Zhao, J.; Dick, B. Recent Development of Heavy-Atom-Free Triplet Photosensitizers: Molecular Structure Design, Photophysics and Application. *J. Mater. Chem. C* **2021**, *9*, 11944–11973.
- (8) Filatov, M. A. Heavy-Atom-Free BODIPY Photosensitizers with Intersystem Crossing Mediated by Intramolecular Photoinduced Electron Transfer. *Org. Biomol. Chem.* **2020**, *18*, 10–27.
- (9) Großkopf, J.; Kratz, T.; Rigotti, T.; Bach, T. Enantioselective Photochemical Reactions Enabled by Triplet Energy Transfer. *Chem. Rev.* **2022**, *122*, 1626–1653.
- (10) Ko, C.-C.; Yam, V. W.-W. Coordination Compounds with Photochromic Ligands: Ready Tunability and Visible Light-Sensitized Photochromism. *Acc. Chem. Res.* **2018**, *51*, 149–159.
- (11) Hamachi, T.; Yanai, N. Recent Developments in Materials and Applications of Triplet Dynamic Nuclear Polarization. *Prog. in Nuclear Mag. Res. Spect.* **2024**, *142–143*, 55–68.
- (12) Nishimura, K.; Kouno, H.; Kawashima, Y.; Orihashi, K.; Fujiwara, S.; Tateishi, K.; Uesaka, T.; Kimizuka, N.; Yanai, N. Materials Chemistry of Triplet Dynamic Nuclear Polarization. *Chem. Commun.* **2020**, *56*, 7217–7232.
- (13) Kagawa, A.; Negoro, M.; Takeda, K.; Kitagawa, M. Magnetic-Field Cycling Instrumentation for Dynamic Nuclear Polarization-Nuclear Magnetic Resonance Using Photoexcited Triplets. *Rev. Sci. Instrum.* **2009**, *80*, 044705.

- (14) Takeda, K.; Takegoshi, K.; Terao, T. Dynamic Nuclear Polarization by Electron Spins in the Photoexcited Triplet State: I. Attainment of Proton Polarization of 0.7 at 105 K in Naphthalene. *J. Phys. Soc. Jpn.* **2004**, *73*, 2313–2318.
- (15) Dance, Z. E. X.; Mickley, S. M.; Wilson, T. M.; Ricks, A. B.; Scott, A. M.; Ratner, M. A.; Wasielewski, M. R. Intersystem Crossing Mediated by Photoinduced Intramolecular Charge Transfer: Julolidine-Anthracene Molecules with Perpendicular π Systems. *J. Phys. Chem. A* **2008**, *112*, 4194–4201.
- (16) Suneesh, C. V.; Gopidas, K. R. Long-Lived Photoinduced Charge Separation Due to the Inverted Region Effect in 1,6-Bis(Phenylethynyl)pyrene-Phenothiazine Dyad. *J. Phys. Chem. C* **2010**, *114*, 18725–18734.
- (17) Ulrich, G.; Ziessel, R.; Harriman, A. The Chemistry of Fluorescent Bodipy Dyes: Versatility Unsurpassed. *Angew Chem Int Ed* **2008**, *47*, 1184–1201.
- (18) Boens, N.; Leen, V.; Dehaen, W. Fluorescent Indicators Based on BODIPY. *Chem. Soc. Rev.* **2012**, *41*, 1130–1172.
- (19) Filatov, M. A.; Karuthedath, S.; Polestshuk, P. M.; Savoie, H.; Flanagan, K. J.; Sy, C.; Sitte, E.; Telitchko, M.; Laquai, F.; Boyle, R. W.; Senge, M. O. Generation of Triplet Excited States via Photoinduced Electron Transfer in *Meso*-Anthra-BODIPY: Fluorogenic Response toward Singlet Oxygen in Solution and in Vitro. *J. Am. Chem. Soc.* **2017**, *139*, 6282–6285.
- (20) Suzuki, K.; Kaji, H. Torsion Angle Analysis of a Thermally Activated Delayed Fluorescence Emitter in an Amorphous State Using Dynamic Nuclear Polarization Enhanced Solid-State NMR. *J. Am. Chem. Soc.* **2023**, jacs.3c05204.
- (21) Sasaki, S.; Drummen, G. P. C.; Konishi, G.-i. Recent Advances in Twisted Intramolecular Charge Transfer (TICT) Fluorescence and Related Phenomena in Materials Chemistry. *J. Mater. Chem. C* **2016**, *4*, 2731–2743.

- (22) Grabowski, Z. R.; Rotkiewicz, K.; Rettig, W. Structural Changes Accompanying Intramolecular Electron Transfer: Focus on Twisted Intramolecular Charge-Transfer States and Structures. *Chem. Rev.* **2003**, *103*, 3899–4032.
- (23) Uoyama, H.; Goushi, K.; Shizu, K.; Nomura, H.; Adachi, C. Highly Efficient Organic Light-Emitting Diodes from Delayed Fluorescence. *Nature* **2012**, *492*, 234–238.
- (24) Dias, F. B.; Penfold, T. J.; Monkman, A. P. Photophysics of Thermally Activated Delayed Fluorescence Molecules. *Methods Appl. Fluoresc.* **2017**, *5*, 012001.
- (25) Tao, Y.; Yuan, K.; Chen, T.; Xu, P.; Li, H.; Chen, R.; Zheng, C.; Zhang, L.; Huang, W. Thermally Activated Delayed Fluorescence Materials Towards the Breakthrough of Organoelectronics. *Advanced Materials* **2014**, *26*, 7931–7958.
- (26) Yang, Z.; Mao, Z.; Xie, Z.; Zhang, Y.; Liu, S.; Zhao, J.; Xu, J.; Chi, Z.; Aldred, M. P. Recent Advances in Organic Thermally Activated Delayed Fluorescence Materials. *Chem. Soc. Rev.* **2017**, *46*, 915–1016.
- (27) Dong, Y.; Sukhanov, A. A.; Zhao, J.; Elmali, A.; Li, X.; Dick, B.; Karatay, A.; Voronkova, V. K. Spin–Orbit Charge-Transfer Intersystem Crossing (SOCT-ISC) in Bodipy-Phenoxazine Dyads: Effect of Chromophore Orientation and Conformation Restriction on the Photophysical Properties. *J. Phys. Chem. C* **2019**, *123*, 22793–22811.
- (28) Sakamoto, K.; Hamachi, T.; Miyokawa, K.; Tateishi, K.; Uesaka, T.; Kurashige, Y.; Yanai, N. Polarizing agents beyond pentacene for efficient triplet dynamic nuclear polarization in glass matrices. *PNAS* **2023**, *120*, e2307926120.
- (29) Miyokawa, K.; Kurashige, Y. Zero-Field Splitting Tensor of the Triplet Excited States of Aromatic Molecules: A Valence Full- π Complete Active Space Self-Consistent Field Study. *J. Phys. Chem. A* **2024**, *128*, 2349–2356.

- (30) Weigend, F.; Ahlrichs, R. Balanced Basis Sets of Split Valence, Triple Zeta Valence and Quadruple Zeta Valence Quality for H to Rn: Design and Assessment of Accuracy. *Phys. Chem. Chem. Phys.* **2005**, *7*, 3297.
- (31) Weigend, F. Accurate Coulomb-fitting Basis Sets for H to Rn. *Phys. Chem. Chem. Phys.* **2006**, *8*, 1057.
- (32) Hellweg, A.; Hättig, C.; Höfener, S.; Klopper, W. Optimized Accurate Auxiliary Basis Sets for RI-MP2 and RI-CC2 Calculations for the Atoms Rb to Rn. *Theor. Chem. Acc.* **2007**, *117*, 587–597.
- (33) Tawada, Y.; Tsuneda, T.; Yanagisawa, S.; Yanai, T.; Hirao, K. A Long-Range-Corrected Time-Dependent Density Functional Theory. *J. Chem. Phys.* **2004**, *120*, 8425–8433.
- (34) Barone, V.; Cossi, M. Quantum Calculation of Molecular Energies and Energy Gradients in Solution by a Conductor Solvent Model. *J. Phys. Chem. A* **1998**, *102*, 1995–2001.
- (35) Neese, F. Software Update: The ORCA Program System—Version 5.0. *WIREs Comput Mol Sci* **2022**, *12*, e1606.
- (36) Zgid, D.; Nooijen, M. The Density Matrix Renormalization Group Self-Consistent Field Method: Orbital Optimization with the Density Matrix Renormalization Group Method in the Active Space. *J. Chem. Phys.* **2008**, *128*, 144116.
- (37) Ghosh, D.; Hachmann, J.; Yanai, T.; Chan, G. K.-L. Orbital Optimization in the Density Matrix Renormalization Group, with Applications to Polyenes and β -Carotene. *J. Chem. Phys.* **2008**, *128*, 144117.
- (38) Yanai, T.; Kurashige, Y.; Ghosh, D.; Chan, G. K.-L. Accelerating Convergence in Iterative Solution for Large-Scale Complete Active Space Self-Consistent-Field Calculations. *Int. J. Quantum Chem.* **2009**, *109*, 2178–2190.

- (39) Ganyushin, D.; Gilka, N.; Taylor, P. R.; Marian, C. M.; Neese, F. The Resolution of the Identity Approximation for Calculations of Spin-Spin Contribution to Zero-Field Splitting Parameters. *J. Chem. Phys.* **2010**, *132*, 144111.
- (40) Sun, Q.; Berkelbach, T. C.; Blunt, N. S.; Booth, G. H.; Guo, S.; Li, Z.; Liu, J.; McClain, J. D.; Sayfutyarova, E. R.; Sharma, S.; Wouters, S.; Chan, G. K.-L. P Y SCF: The Python-based Simulations of Chemistry Framework. *WIREs Comput Mol Sci* **2018**, *8*.
- (41) Caricato, M.; Mennucci, B.; Tomasi, J.; Ingrosso, F.; Cammi, R.; Corni, S.; Scalmani, G. Formation and Relaxation of Excited States in Solution: A New Time Dependent Polarizable Continuum Model Based on Time Dependent Density Functional Theory. *The Journal of Chemical Physics* **2006**, *124*, 124520.
- (42) Chibani, S.; Laurent, A. D.; Le Guennic, B.; Jacquemin, D. Improving the Accuracy of Excited-State Simulations of BODIPY and Aza-BODIPY Dyes with a Joint SOS-CIS(D) and TD-DFT Approach. *J. Chem. Theory Comput.* **2014**, *10*, 4574–4582.
- (43) Hansch, Corwin.; Leo, A.; Taft, R. W. A Survey of Hammett Substituent Constants and Resonance and Field Parameters. *Chem. Rev.* **1991**, *91*, 165–195.



KYOTO UNIVERSITY

Yuki Kurashige

Department of Chemistry,
Graduate School of Science,
Kyoto University
Mail: kura@kuchem.kyoto-u.ac.jp

The data supporting this study's findings are available from the corresponding authors upon reasonable request.